

Pattern Analysis in Dermoscopic Images

Aurora Sáez, Begoña Acha and Carmen Serrano

Abstract In this chapter an extensive review of algorithmic methods that automatically detect patterns in dermoscopic images of pigmented lesions is presented. Pattern Analysis seeks to identify specific patterns, which may be global and local. It is the method most commonly used for providing diagnostic accuracy for cutaneous melanoma. In this chapter, a description of global and local patterns identified by pattern analysis is presented as well as a brief explanation of algorithmic methods that carry out the detection and classification of these patterns. Although the 7-Point Checklist method corresponds to a different diagnostic technique than pattern analysis, it can be considered as a simplification of it as it classifies seven features related with local patterns. For this reason, the main techniques to automatically assess the 7-Point Checklist are briefly explained in this chapter.

Keywords Pattern analysis · Dermoscopy · Texture descriptors · Local patterns detection · Global patterns detection · Classification · Machine learning

Introduction

The medical term melanoma refers to a malignant tumor developed from melanocytic cells. Melanoma generally appears de novo, and less frequently as the evolution of acquired benign melanocytic nevi. In the last decades, mainly due to sun exposure,

A. Sáez (✉) · B. Acha · C. Serrano
Dpto. Teoría de la Señal y Comunicaciones, Universidad de Sevilla. Camino de los Descubrimientos s/n, Seville, Spain
e-mail: aurorasaez@us.es

B. Acha
e-mail: bacha@us.es

C. Serrano
e-mail: cserrano@us.es

the incidence of melanoma has dramatically increased, particularly in young white population. If diagnosed and treated early, the mean life expectancy of individuals suffering from melanoma can be increased by at least 25 years [11].

A non-invasive technique to assist dermatologists in the diagnosis of melanoma is dermoscopy, which is an epiluminescence light microscopy, that magnifies lesions and enables examination down to the dermo-epidermal junction. There are four main diagnosis methods from dermoscopic images: ABCD rule, pattern analysis, Menzies method and 7-Point Checklist. These methods were evaluated during the 2,000 Consensus Net Meeting on Dermoscopy (CNMD) [5] by experts from all over the world. A 2-step procedure was used to facilitate the diagnosis:

1. To decide whether the lesion is melanocytic or non-melanocytic.
2. To decide whether the melanocytic lesion is benign, suspect, or malignant.

Pattern Analysis, considered as the classic approach for diagnosis in dermoscopic images, was deemed superior to the other algorithms. The favorable results of pattern analysis were not unexpected, because this method probably reflects best the way the human brain is working when categorizing morphological images [5]. Pattern Analysis, set forth by Pehamberger and colleagues in 1987 [36], was updated by the Consensus Net Meeting of 2000 [5]. This methodology defines the significant dermatoscopic patterns of pigmented skin lesions. Currently, it is the method most commonly used for providing diagnostic accuracy for cutaneous melanoma [38].

Pattern Analysis seeks to identify specific patterns, which may be global or local. The global features allow a quick preliminary categorization of a given pigmented skin lesion prior to more detailed assessment, and they are presented as arrangements of textured patterns covering most of the lesion. The local features represent individual or grouped characteristics that appear in the lesion. Some conclusions from this methodology were extracted in the consensus mentioned [5]; the global feature most predictive for the diagnosis of melanoma was the multicomponent pattern, whereas the globular, cobblestone, homogeneous, and starburst patterns were most predictive for the diagnosis of benign melanocytic lesions. Regarding to local features, atypical pigmented network, irregular streaks, and regression structures were the features that showed the highest association with melanoma, followed by irregular dots/globules, irregular blotches, and blue-whitish veil. Vascular structures were not found to be significantly associated with melanoma. On the contrary, typical pigmented network, regular dots/globules, regular streaks, and regular blotches were mostly associated with benign melanocytic lesions.

Although the 7-Point Checklist method corresponds to a different diagnostic technique than pattern analysis, it can be considered as a simplification of it, as it classifies seven features related with local patterns [3]. Such simplified algorithm was designed to prevent non-experts from missing the detection of melanomas, even at the cost of decreased specificity.

Due to the proven benefits of applying digital imaging to dermatology [5, 49], image processing research has directed a strong effort to develop Computer Aided Diagnosis (CAD) tools to assist physicians in their task of analyzing pigmented lesions, especially because a dermatologist is not always the physician that analyzes

them in a first trial. In 2009 Maglogianis and Doukas [33] presented an overview of CAD systems, describing how to extract features through digital image processing methods and techniques for skin lesion classification. The special issue -Advances in skin cancer image analysis [14]—edited by Celebi, Stoecker and Moss in 2011 summarized the progress that has taken place in this field, including works related to multispectral imaging system, enhancement of dermoscopy images, detection of lesion border and feature extraction. And the recent work from Korotkov and Garcia [31] presents an extensive review of computerized analysis of pigmented skin lesions applied to microscopic (dermoscopic) and macroscopic (clinical) images.

In this chapter an exhaustive review of methods devoted to quantify features in pattern analysis is presented. A brief summary of the main techniques focused on the extraction of local patterns [2, 13, 30, 34, 42, 43, 45], including those that quantify the 7-Point Checklist [8, 9, 17, 19, 20], will be presented in section “Local Pattern Analysis”. Section “7-Point Checklist Method” will be devoted to explain the main algorithms that implement the 7-Point Checklist method. When dealing with the detection and/or classification of global patterns, a few methods have been published in the literature [1, 25, 40, 44]. In section “Global Pattern Analysis” a description of these methods is introduced, describing in detail Serrano’s work [44], where reticular, globular, cobblestone, homogeneous and parallel patterns are classified.

Local Pattern Analysis

The presence of specific dermoscopic features in different regions of the same lesion contributes to make a diagnosis of melanocytic lesions and are called local patterns. They are dermoscopic structures such as pigment network, dots and globules, streaks, blue-whitish veil, regression structures, hypopigmentation and vascular structures, whose appearance description is presented below [4]. The predominant presence of some of these local patterns can determine some global patterns [4, 5].

- Pigment network. Delicate, regular grid of brownish lines over a diffuse light-brown background.
- Dots/globules. Sharply circumscribed, usually round or oval, variously sized black, brown or grey structures.
- Streaks. Brownish-black linear structures of variable thickness.
- Blue-whitish veil. Grey-blue to whitish-blue, diffuse pigmentation associated with pigment network alterations, dots/globules and/or streaks.
- Pigmentation. Dark-brown to grey-black, diffuse area that precludes recognition of more subtle dermoscopic features such as pigment network or vascular structures.
- Hypopigmentation. Diffuse area of decreased pigmentation within an otherwise ordinary pigmented lesion.
- Regression structures. White areas, blue areas and a combination of both. Virtually indistinguishable from the blue-whitish veil.
- Vascular structures.

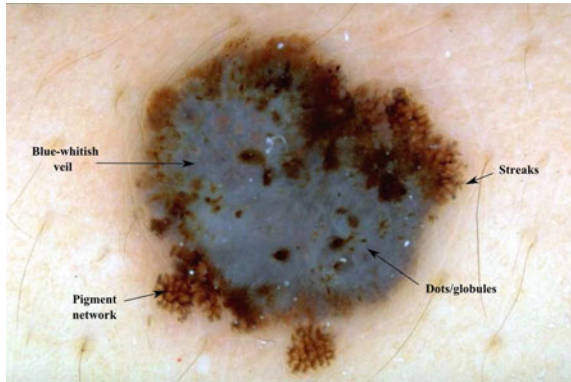


Fig. 1 Example of local patterns

- Other criteria, such as milia-like cysts, comedo-like openings, blotches, Lacunas network, etc.

Local patterns can be presented in the lesion with an irregular/regular or atypical/typical nature, implying malignancy or not. Figure 1 shows some examples of local patterns.

In the literature we can find numerous works that are focused on the automatic identification of local features. They are briefly explained in the subsections below.

Pigment Network

The pigment network is the most studied local pattern. The reason is that it is the most common local pattern in melanocytic lesions, and the identification of melanocytic lesions is the first step in the procedure of pigmented skin lesion diagnosis as explained in the Introduction Section. A pigment network can be typical, when the pattern is regularly meshed, narrowly spaced and its distribution is more or less regular, or atypical, characterized by a black, brown, or grey, irregular network, distributed irregularly throughout the lesion. An atypical network signals malignancy [4]. Figure 2 shows the variability of its appearance.

In the last years several authors have focused on the automatic detection of this pattern.

Anantha et al. [2] in 2004 compared two statistical texture identification methods for detecting the pigment network. The first method was the neighboring grey-level dependence matrix (NGLDM), and the second method used the lattice aperture wave-form set (LAWS). They analyzed images of 64×64 pixels. The authors concluded that both methods detect grossly any pigment network with reasonable accuracy, with slightly better results obtained by the latter. 155 dermoscopic images were analyzed,

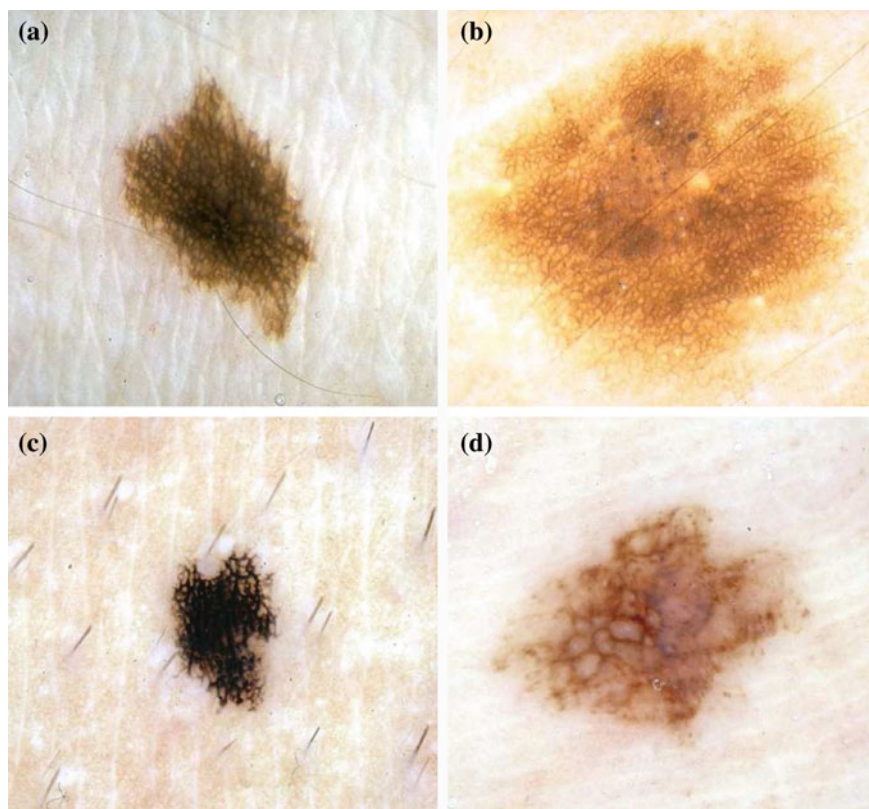


Fig. 2 Example of lesions with pigment network. **a** and **b** present typical pigment network, whereas **c** and **d** atypical

including 62 malignant melanomas and 93 benign lesions. The success classification percentage was around 78 % and 65 % for LAWS and NGLDM, respectively.

Grana et al. [23] in 2006 presented an approach that addressed the problem of detecting the pigment network based on the work of linear structure identification presented in [48], applied to dermatological images by Fleming et al. [21] in 1998. Line points detection was satisfied considering the lines of the pigment network as ridges. As a consequence this set of points must satisfy at the same time two conditions: the first order derivative should be zero, while the second order derivative should have a high module value. After the detection of lines from the zeros of the first derivative, Fleming et al. [21], following the procedure presented in [48], closed lines through an analysis of the second derivative. However, Grana et al. [23] made use of a set of morphological masks that rotate in different directions in order to identify the terminations of the lines and, subsequently, line linking. The thinning approach worked by selectively eroding line points which matched with exactly only one of the morphological masks checking for the presence of an 'L' shaped point

which is not an 8-connection between two different network segments. ‘T’ shaped connections were eroded with another set of masks. After the network extraction, the image was divided into eight sectors oriented along the principal axes, in order to provide some statistics on the network characteristics of the whole lesion and of every eighth thereof counting the number of meshes, along with the number of unclosed terminations and the average line width. A set of 60 selected lesions was examined. Interestingly, the authors classified each lesion with regard to the distribution of the pigment network as no network pattern, partial network pattern if the lesion is partially covered with pigment network and complete network pattern. An overall 88.3 % network detection performance, without failed detections, was achieved.

Shrestha et al. [45] presented a study in 2010, whose purpose was to identify a method that could discriminate malignant melanoma with an irregular texture, most commonly an atypical pigment network (APN), from benign dysplastic nevi, which generally do not have an APN, using texture measurements alone. In this study, a gray-level co-occurrence matrix (GLCM) is constructed from the luminance plane. Five different GLCMs were constructed for each image using pixel distances (d-values) of 6, 12, 20, 30, and 40. Five classical statistical texture measures were calculated from each GLCM: energy, inertia, correlation, inverse difference, and entropy. Both the average and the range of each of these measures were computed, yielding 10 parameters related to texture. These parameters fed six different classifiers (BayesNet, ADTree, DecisionStump, J48, NBTree, and Random Forest) in order to determine whether an image presented pigment network or not. The method was tested with 106 dermoscopy images including 28 melanomas and 78 benign dysplastic nevi. The dataset is divided into APN areas and non-APN area. 10-fold validation is employed to validate the method. The correlation average provided the highest discrimination accuracy (95.4 %). The best discrimination of melanomas is attained for a d-distance of 20.

Sadeghi et al. [42] proposed a method to detect and classify the dermoscopic structure pigment network. The method was based on the detection of the ‘holes’ of the network and follows the next steps: image enhancement, pigment network detection, feature extraction, and classification in three classes. First, a two-dimensional high-pass filter was applied to highlight texture features. Then, the lesion was segmented using Wighton et al. method [54] which employed supervised learning and the random walker algorithm. In the pigment network detection step, a Laplacian of Gaussian (LOG) filter was used to detect sharp changes of intensity. Then, the resulting binary image was converted into a graph using 8-connected neighbouring. Cyclic structures were found in this graph, and noise or undesired cycles were removed. Lines and holes of the pigment network were identified and 69 clinically inspired features were extracted: 20 structural features, including network thickness and its variation within the lesion, as well as size of the holes and its variation along the network; 2 geometric features to study the ‘uniformity’ of the network; 37 chromatic features; and 10 textural features, using the five classical statistical texture measurements, also proposed in [45]. This allowed to classify the network into typical or atypical type. These 69 features were fed into a classifier based on a powerful boosting algorithm LogitBoost. A dataset consisting of 436 images (161 Absent, 154

Typical network, 121 Atypical network) was used. The authors computed results for both the 3-class (Absent, Typical or Atypical) and 2-class problems (Absent, Present). Ten-fold cross validation was used to generate all results. An accuracy of 82 % discriminating between three classes and an accuracy of 93 % discriminating between two classes were achieved. In [43], the same authors, according to the density of the pigment network graph, classified a given image into Present or Absent. The method was evaluated with 500 images obtaining an accuracy of 94.3 %.

In 2011 Wighton et al. [53] proposed the use of supervised learning and MAP estimation for automated skin lesion diagnosis. The authors applied this method to three task: segmentation, hair detection and identification of pigment network. The method was divided into three main steps. First, in a feature extraction stage, images were converted to CIE $L^*a^*b^*$ [37], and each color channel was filtered with a series of Gaussian and Laplacian of Gaussian filters at various scale ($\sigma = 1.25, 2.5, 5, 10, 20$), so that a total of 30 features were obtained for each pixel. Secondly, after feature extraction, Linear Discriminant Analysis (LDA) was used to reduce the dimensionality. Finally, the posterior probabilities $P(p|l_i)$ ($p = pixel$, $l_i = class$) in this subspace were modelled as multivariate Gaussian distributions. In the training phase, parameters for multivariate Gaussian distributions of each class were estimated. And in the labelling stage, individual pixels from previously unseen images were assigned a label using MAP estimation. A training dataset consisting in 20 images where pigment network was present across the entire lesion and 20 images absent of pigment network was employed. All the images belonged to the dermoscopy atlas presented in [4], where labels of ‘present’ or ‘absent’ of pigment network are supplied for each image. Pixels from the training images were assigned a label as ‘background’, ‘absent’ or ‘present’. To label a new unseen image, features were computed as in the training phase and the dimensionality of the feature space is reduced. To estimate the probability that a pixel p was labelled l_i ($P(l_i|p)$) the authors assigned the most probable label according to MAP estimation.

Skrovseth et al. [47] also proposed a pattern recognition technique with supervised learning to identify pigment network. They selected a training set consisting of a large number of small images containing either a sample of network or a sample of other textures, consisting of both skin and lesion regions. 20 different texture measures were analyzed and the three that contributed maximally to separate the two classes with a linear classifier were selected. A new image is divided into overlapping subimages of the same size as the training images. A pixel is classified as network if at least one of the subimages it belongs to is classified as it.

Barata et al. [7] presented a work focused on the detection of pigment network in 2012. The method was based on the use of directional filters. The first step was to convert the color image into a grey scale one to remove two types of artifacts: hair and reflections caused by the dermatological gel. An inpainting technique was applied. In the second step, regions with pigment network were detected using two of its distinctive properties: intensity and geometry or spatial organization. A bank of directional filters was applied to perform an enhancement of the network. The spatial organization was implemented by connectivity among pixels. The result was a binary net-mask. The final step aimed to assign a binary label to each image: with or

without pigment network. To accomplish this objective, features which characterize the topology of the detected regions in a given image were extracted and used to train a classifier using a boosting algorithm. The algorithm was tested on a dataset of 200 dermoscopic images (88 with pigment network and 112 without) achieving a sensitivity of 91.1 %, a specificity of 82.1 % and an accuracy of 86.2 % in the classification with or without pigment network.

Betta et al. [9] proposed a method for the detection of atypical pigment network. The method was based on their previous work [8], where the pigment network was detected but not classified as atypical/typical. The authors combined two different techniques: structural and spectral analysis. The structural analysis searched for primitive structures such as lines and/or points. To identify these local discontinuities the monochromatic image was compared with a median filtered version of it. In the spectral analysis the Fourier transform of the monochromatic image was performed in order to determine the spatial period of the texture. In this way, local discontinuities, not clearly associated with the network, were disregarded. The result of this phase was a ‘regions with network’ mask. This mask in conjunction with ‘local discontinuities’ image provided a ‘network image’, where the areas belonging to the lesion and constituting the pigment network were highlighted. Two indices related to the spatial and chromatic variability of these areas were presented to quantify the possible atypical nature of the network. 30 images were processed to assess the performance of this detection.

Di Leo et al. [19] extended the work proposed by Betta et al. [9] to detect atypical pigmented network. First, the pigment network was detected following [9]. Then, 13 color and geometric features were extracted. C4.5 algorithm was used as classifier. 173 digital dermoscopy images (77 atypical pigment network, 53 typical pigment network and 43 absent pigment network) obtained from the Interactive Atlas of Dermoscopy [4] were used. 90 images were used for training and 83 images for testing. Sensitivity and specificity values greater than 85 % were reached.

In Table 1 the classification results of the works reported in this section are summarized.

Table 1 Results of pigment network detection

Algorithm	Year	Classification	Accuracy (%)	No. images
Anantha et al. [2]	2004	Absent/present	78	155
Grana et al. [23]	2006	No/Partial/complete	88.3	60
Shrestha et al. [45]	2010	Melanoma/no	95.4	106
Sadeghi et al. [42]	2010	Absent/present	93	436
Sadeghi et al. [42]	2010	Absent/atypical/typical	82	436
Skrovseth et al. [47]	2010	Absent/present (per-pixel)	–	–
Wighton et al. [53]	2011	Absent/present (per-pixel)	–	734
Barata et al. [7]	2012	Absent/present	86.2	200
Betta et al. [9]	2006	Atypical/typical	–	30
Di Leo et al. [19]	2008	Atypical/typical	85	173

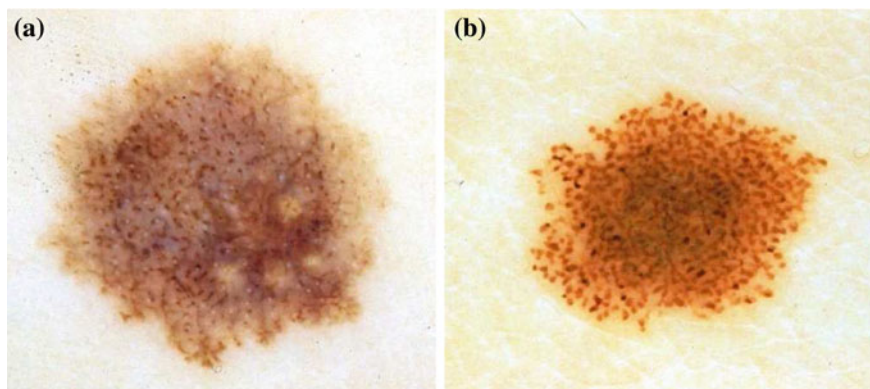


Fig. 3 Example of lesions with *dots/globules*

Table 2 Results of *dots/globules* detection

Algorithm	Year	Classification	Accuracy	No. images
Yoshino et al. [56]	2004	Absent/Present	–	–
Skrovseth et al. [47]	2010	Absent/Present	–	–

Dots and Globules

Dots and globules are round or oval, variously sized black, brown or grey structures, as it has already mentioned in Local Pattern Analysis. It is another dermoscopic structure which is difficult to discriminate from pigment network [42]. This could be the reason why there are so few works in the literature focused on its identification. Some examples of lesions with this structures are shown in Fig. 3.

Based on the classification described in [35], Skrovseth et al. [47] computed a score for each pixel in a gray scale image. Given P surrounding pixels with values g_k , $k = 1, \dots, P$ at a radius R of a central pixel with gray value g_c , the score of the central pixel is calculated as $S_c = \sum_{k=1}^P (g_c - g_k)$. The authors argue that this score will be large for a dark spot, and therefore, a simple thresholding would give the position of the dot.

Yoshino et al. [56] presented an algorithm that use morphological closing operation to detect dots. The closing operation used a linear structural element. Afterwards, a thresholding is applied to detect dots.

Table 2 shows a summary of the works focused on the globules detection.

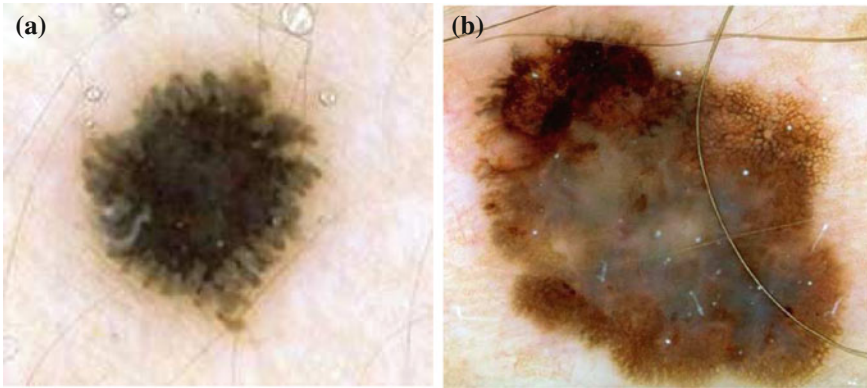


Fig. 4 Example of lesions with (a) regular streaks, (b) irregular streaks

Streaks

Streaks are brownish-black linear structures of variable thickness that are found in benign and malignant lesions. They are typically placed at the periphery of a lesion and are not necessarily connected to the lines of the pigment network. Streaks can be irregular, when they are unevenly distributed (malignant melanoma), or regular (symmetrical radial arrangement over the entire lesion) [10]. An example of regular and irregular streaks can be found in Fig. 4 .

Mirzaalian et al. [34] proposed a machine-learning approach to detect streaks which captures the quaternion tubularness in the color dermoscopic images. First, tubularness filters [22] to enhance streak structures in dermoscopic images were used. Given the estimated tubularness and direction of the streaks, a vector field in order to quantify radial streaming pattern of the streaks was defined. Specifically, they computed the amount of flux of the field passing through iso-distance contours of the lesion, where each contour was the loci of the pixels which have equal distance from the outer lesion contour. So, an appearance descriptor based on the mean and variance of the flux through the different concentric bands of the lesion is constructed. The final step is to learn how the extracted descriptors can best distinguish the three different classes: the absence, presence of regular, or presence of irregular streaks in the dermoscopic images. This task is performed with a SVM classifier with a database 99 dermoscopic images.

In [41], the authors followed four steps to locate streaks: preprocessing, blob detection, feature selection and two-class classification (absent-present). In the preprocessing step, lesions were segmented, reoriented so that the major axis was parallel to the x-axis and resized so that its major axis occupied 500 pixels. Lightness component (L^*) from $L^*a^*b^*$ color representation was used for the rest of the analysis. Streaks can be modeled as linear structures with a Gaussian cross-section profile near the border. Therefore, in the blob detection, four Laplacian of Gaussian (LOG) filters

with different sizes, $hsize = 3, 5, 7, 9$, were employed to detect these linear structures. Candidate streaks were extracted in this step. Once they were detected, their orientations were estimated using the Averaged Squared Gradient Flow (ASGF) algorithm [29]. Then, 25 features were extracted from the candidate linear streak structures and from the lesion: one set of 12 features was based on properties of the detected candidate streak lines and another feature set contained the 13 common color and texture features of the entire lesion. These 25 features were fed to a SimpleLogistic classifier, that classifies a lesion into absence and presence of streaks. The method was tested with a database of 300 dermoscopic images (105 Absent and 195 Present) achieving an accuracy detection of 0.815 using 10-fold cross validation.

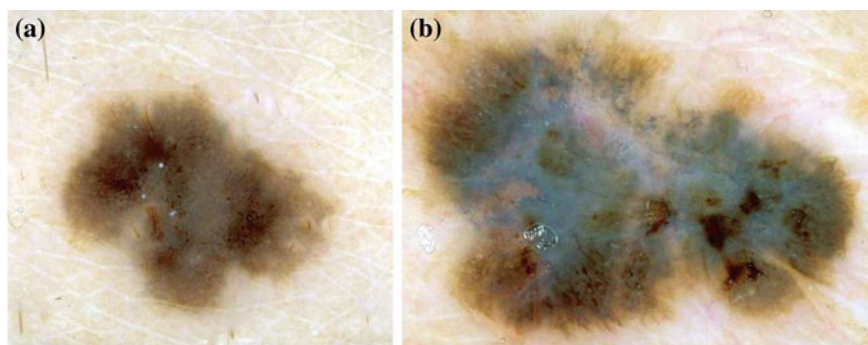
Sadeghi et al. [39] recently presented an extension of their previous work [41]. In this version, they proposed an algorithm that classifies a lesion into absence of streaks, regular streaks, and irregular streaks. The work aimed to identify valid streak lines from the set of candidate streak lines obtained in [41] in order to reduce false positive streaks such as hairs and skin lines. The method also extends the analysis to identify the orientation and spatial arrangement of streak lines. These novel geometric features are used to identify not only the presence of streak lines, but whether or not they are Irregular or Regular; important for melanoma diagnosis. Therefore, a total of 31 features are fed into a classifier, achieving an accuracy of 76.1 % when classifying 945 images into the three classes.

Betta et al. [8] identified streaks as finger-like irregularities with uniform brown color at the lesion contour. Therefore, they detected the simultaneous occurrence of two different structures: finger-like track of the lesion contour, and brown pigmentation in the same restricted region. For the first purpose, the color image was converted to an 8-bit gray-level image, and then three different binary images were obtained by applying three different thresholds. The contours of these binary images were extracted by a blob-finding algorithm. The best of the three extracted contours was selected manually and divided into 16 parts. For each part, an irregularity ratio was evaluated. This parameter represented the ratio between number of pixels of the detected contour in this part and the number of pixels in the line connecting the extreme contour points of this part. The contour in that region was assumed as irregular if the ratio was greater than a threshold. On the other hand, brown pigmentation of those 16 subimages is analyzed by thresholding the hue component. Finally, the occurrence of streaks was assumed only if both an irregular contour and a brown pigmentation were found in the same sub-image. The authors presented experimental results for 10 images achieving a 90 % of success rate. A further evaluation was presented by Fabbrocini et al. [20]. They used 23 and 30 images for training and test set, respectively. The two thresholds mentioned above were determined by a Receiver Operating Characteristic curve (ROC curve) on the training image set. A sensitivity and a specificity of 86 and 88 %, respectively, were achieved.

Table 3 summarizes the classification results of the works reported in this section.

Table 3 Results of **streaks** detection following pattern analysis and 7-Point Checklist

Algorithm	Year	Classification	Accuracy (%)	No. images
Mirzaalian et al. [34]	2012	Absent/regular/irregular	91	99
Sadeghi et al. [39]	2013	Absent/present	78.3	945
Sadeghi et al. [39]	2013	Absent/regular/irregular	76.1	945
Betta et al. [8]	2005	Absent/present	90	10
Fabbrocini et al. [20]	2010	Absent/present	86	30

**Fig. 5** Example of lesions with *blue–whitish veil*

Blue–Whitish Veil

Blue-whitish veil is characterized by a grey-blue to whitish-blue diffuse pigmentation. Some examples of lesions that present this pattern are shown in Fig. 5.

Celebi et al. [13] proposed a machine learning approach to detect blue-white veil in dermoscopy images based on their early work [12]. Fifteen color features and three texture features were extracted. The color features involved absolute color features and relative color features when compared to the average color of the background skin. The texture features were based on the gray level co-occurrence matrix (GLCM). The classifier used was C4.5 algorithm. Only 2 out of the 18 features were finally selected for the classification model, both belonging to color features. The classification results for manually selected test pixels yield a sensitivity of 84.33 % and a specificity of 96.19 %. In a second experiment, the authors aimed to discriminate between melanoma and benign lesions based on the area of the blue–white veil detected. They extracted three numeric values from the detected blue-white region: area, circularity and ellipticity. A new classification model based on these features was generated using C4.5 algorithm and 10-fold-cross validation. A sensitivity of 69.35 % and a specificity of 89.97 % for the entire image set (545 images) were obtained.

In a recent work, Arroyo et al. [6] also proposed supervised machine learning techniques to detect blue-white veil. To this aim, color features were extracted from

Table 4 Results of **blue-whitish veil** detection

Algorithm	Year	Classification	Sensitivity (%)	Specificity (%)	No. images
Celebi et al. [12]	2006	Absent/present (per pixel)	84.33	96.19	100
Celebi et al. [13]	2008	Melanoma/Benign	69.35	89.97	545
Arroyo et al. [6]	2011	Melanoma/Benign	80.50	90.93	887
Di Leo et al. [17]	2009	Absent/present	87	85	135

each individual pixel and the classifier used was C4.5 algorithm, that generated the decision tree. Candidate areas selected in the previous step were subsequently classified as melanoma with blue-white veil. For this purpose 12 features were extracted from the candidate area such as area, solidity or ellipticity. The authors used a database consisting of 887 images. 120 images were selected to obtain the training data, 60 corresponding to melanoma with blue-white veil pattern and 60 corresponding to other cases. The method achieved a sensitivity of 80.50 % and a specificity of 90.93 %

Di Leo et al. [17] focused on the detection of two different patterns, blue-whitish veil and regression structures. Firstly, the lesion was subdivided into regions. The color image is converted via principal component analysis (PCA) and a two dimensional (2-D) histogram is computed with the two first principal components. The most significant peaks in the 2-D histogram were found as representative of color regions in the input image. All the pixels in the lesion were assigned to one the main peaks via clustering, so that a lesion map was created. Regions in the lesion map were subsequently classified as present or absent of blue whitish veil and regression. To this aim geometric and color features were extracted and a logistic model tree (LMT) was proposed as classifier. 210 digital dermoscopic images obtained from the Interactive Atlas of Dermoscopy [4] were used. 70 and 50 cases corresponding to the presence of Blue Veil and Regression area respectively were used as training set. 65 cases of Blue Veil and 40 cases of Regression structures were utilized for the test set. A sensitivity of 0.87 and a specificity of 0.85 were obtained for the detection of blue veil and a sensitivity and a specificity both equal to 0.85 for regression structures.

Table 4 shows the classification results of the mentioned works.

Blotches

Blotches are dark structureless areas within pigmented lesions [5]. Blotches that are located asymmetrically within a lesion are indicative of malignant melanoma [30].

The chapter of Stoecker et al. [50] studied the effectiveness of the absolute and relative color blotch features for melanoma/benign lesion discrimination over a dermoscopy image set containing 165 melanomas and 347 benign lesions using a neural network approach. The authors proposed two approaches to detect the blotchy areas. The first method used thresholds placed upon the values of the red, green, and blue (RGB) components of the pixels within the lesions. The second method used

relative color thresholds, subtracting the observed pixel value within the lesion from the background skin color before applying relative thresholds. Then, several blotch indices were computed, including the scaled distance between the largest blotch centroid and the lesion centroid, ratio of total blotch areas to lesion area, ratio of largest blotch area to lesion area, total number of blotches, size of largest blotch, and irregularity of largest blotch. It was determined that relative color were more effective than absolute color giving a diagnostic accuracy of about 77 %.

Khan et al. [30] investigated new and existing blotch features for melanoma discrimination. Four experiments were performed to achieve this aim. Blotches are first extracted using absolute and relative color thresholds to construct blotch masks proposed in [50]. Then, fuzzy logic techniques for extracting blotches based on blotch size were studied, where a fixed minimum blotch size was fuzzified to detect an area as a blotch only if its size exhibits a certain degree of association with a fuzzy set representative of blotch size. To compute the second fuzzy set, the relative color values at each pixel position inside of the blotchy areas were extracted from melanoma lesions belonging to a training set of images. This fuzzy set provided the basis for differentiating between melanoma and benign skin lesions. A third fuzzy set was constructed similarly, but using separate relative color histograms for the red, green and blue color planes. These sets were also used for melanoma discrimination. Finally, a new set of four asymmetry features were computed. The lesion border mask was divided into four quadrants and a set of asymmetry features was computed. The work concluded that features computed from blotches using the fuzzy logic techniques based on three plane relative color and blotch size yielded the highest diagnostic accuracy of 81.2 %. 424 dermoscopy images (134 melanoma and 290 benign images) from three different sources were used.

Madasu and Lovell [32] proposed an extension of fuzzy co-clustering algorithm for images (FCCI) technique [24] for detecting blotches. Madasu and Lovell extended FCCI technique to include texture features as additional clustering parameters. Texture features were computed using the normalized entropy function. A set of 50 images were used for testing the proposed algorithm. The authors claimed that the blotches are accurately located independently of their shape, size or location within the image.

A summary of classification results of the three works presented is shown in Table 5.

Table 5 Results of **blotches** detection

Algorithm	Year	Classification	Accuracy (%)	No. images
Stoecker et al. [50]	2005	Melanoma/Benign	77	512
Khan et al. [30]	2008	Melanoma/Benign	81.2	424
Madasu and Lovell [32]	2009	Absent/Present	–	50

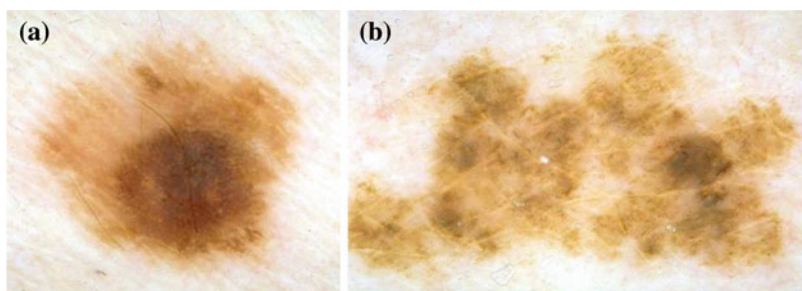


Fig. 6 **a** Nevus with hypopigmentation. **b** Melanoma with hypopigmentation

Table 6 Results of **hypopigmentation** detection

Algorithm	Year	Classification	AUC (%)	No. images
Dalal et al. [15]	2011	Melanoma/Benign	95.2	244

Hypopigmentation

Hypopigmentation represents a diffuse area of decreased pigmentation within an otherwise ordinary pigmented lesion. White areas in a melanoma have an eccentric location and an irregular shape. White areas in a nevus are located in the lesion periphery.

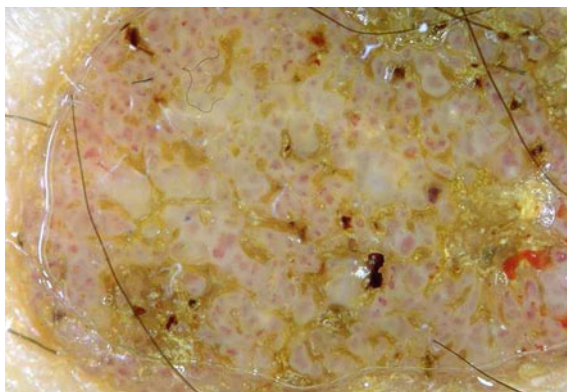
Dalal et al. [15] proposed a method to discriminate melanomas from benign nevi by automatically detecting white areas and measuring features of these white areas. In order to identify white and hypopigmented areas, thresholds were determined for each color plane based on color histogram analysis using a training set of images. The lesion was segmented in concentric deciles. Overlays of the white areas on the lesion deciles were determined. Nine indices were calculated to characterize the automatically detected white areas in a lesion. These indices included lesion decile ratios, normalized number of white areas, absolute and relative size of largest white area, relative size of all white areas, and white area eccentricity, dispersion, and irregularity. A neural network was selected as classifier. 244 benign and malignant dermoscopy images with white areas were selected. The methods used a randomly selected training set of 75 lesions and a test set of 169 lesions.

Regression Structures

A regression structure is a white scarlike depigmentation irregularly distributed within the lesion.

Table 7 Results of **regression structures** detection

Algorithm	Year	Classification	Sensitivity (%)	Specificity (%)	No. images
Di Leo et al. [17]	2009	Absent/present	85	85	90

Fig. 7 Example of lesion with *dotted* vessels

As mentioned above, Di Leo et al. in their work [17] detected regression structures and blue-whitish veil. The method is reported in section “Local Pattern Analysis”. Table 7 shows the classification result of this work.

Vascular Pattern

A vascular pattern, and more specifically, with atypical nature presents linear-irregular or dotted vessels not clearly combined with regression structures and associated with pigment network alterations, dots/globules and/or streaks.

In Betta et al. work [9], reported in section “Pigment Network”, a method for the detection of atypical vascular pattern is also proposed. Due to its difficult to obtain a relevant number of ELM images with the occurrence of this criterion, the training set was constituted by N pixels selected as vascular patterns in a set of images containing occurrences of this criterion. The Hue, Saturation and Luminance components was evaluated and the frequency histograms corresponding to the three color planes were determined. The pixel classification depended on the value of its HSL components. However, the authors warned that in some cases the algorithm gave rise to wrong detection, evidencing a low specificity.

General Feature Extraction

Situ [46] formulate the problem of local dermoscopic feature detection as a multi-instance learning (MIL) problem and not as the identification of each local pattern. The first step was to segment each lesion image into five homogeneous regions by the graph cut method. Each of these regions was considered an instance. In a standard multi-instance learning (MIL) problem a lesion is positive if and only if at least one of its instances is positive. The authors employed the method of diverse density (DD) and evidence confidence (EC) function to convert MIL to a single-instance learning (SIL) problem. Both texture and color descriptors were extracted and a SVM classifier was used. The performance of this MIL approach was compared with its boosting version and a baseline method without using MIL, where the descriptors were extracted from the whole lesion. The authors concluded that MIL methods can be helpful in recognizing certain local features that are important for melanoma detection.

7-Point Checklist Method

Although the 7-Point Checklist method is a different diagnosis algorithm, it is considered a simplification of the classic pattern analysis due to the low number of features to identify. This algorithm is applied once the lesion is diagnosed as melanocytic. It was developed by Argenziano et al. [3]. The 7-Point Checklist is a score system. This method uses seven specific criteria for melanoma. It includes three major criteria:

- Atypical pigment network
- Blue-whitish veil
- Atypical vascular pattern

to which 2 points are attributed to each of them, and four minor criteria:

- Irregular streaks
- Irregular pigmentation
- Irregular dots/globules
- Regression structures

to which 1 point is attributed to each of them. A score of 3 or greater is associated with a high likelihood of melanoma diagnosis at pathology evaluation.

Some works focused on the detection of one or several specific criteria can be found in the literature [8, 9, 17, 19, 20]. These works have been explained in section “Local Pattern Analysis”.

Di Leo et al. in [18] and [16], joined some methods also mentioned in section “Local Pattern Analysis” in order to present an automatic implementation of the 7-Point Checklist method. In [18] the authors focused on the detection of five criteria. It is in [16] where the seven criteria of the method were addressed: Atypical pigment

network and Irregular dots/globule were detected by the methods proposed in [19] and [9]; Blue-whitish veil, Regression structures and Irregular pigmentation detection followed the steps proposed in [17]; atypical vascular pattern was detected with [9]; and Irregular streaks with the method presented in [8]. 300 images were used for the evaluation. For each dermoscopic criterion a training and testing set were selected from the database in order to train a classifier and/or carry out a statistical analysis. The system distinguished between Melanoma and Benign lesions. The performance of the automatic system was estimated through a comparison with the application of the 7-Point Checklist diagnostic method by expert dermatologists to 287 images of the database. The global sensitivity and specificity values of the software diagnostic tool were 0.83 and 0.76, respectively.

Other authors [11, 26] focused their works on machine learning approaches, where the feature extraction step was inspired on the 7 point checklist criteria.

Global Pattern Analysis

Global features allow a quick preliminary categorization of a given pigmented skin lesion prior to more detailed assessment, and they are presented as arrangements of textured patterns covering most of the lesion.

The main global patterns are [4]:

- Reticular pattern. The most common global feature in melanocytic lesions is characterized by a pigment network covering most parts of a given lesion. Basically, the pigment network appears as a grid of thin brown lines over a diffuse light brown background.
- Globular pattern. It is characterized by the presence of numerous, variously sized, round to oval structures with various shades of brown and grey-black coloration.
- Cobblestone pattern. It is quite similar to the globular one but is composed of closely aggregated, larger somewhat angulated globules resembling a cobblestone.
- Homogeneous pattern. It appears as a diffuse, brown, grey-blue to grey-black or reddish-black pigmentation in the absence of pigmented network or other distinctive local features.
- Starburst pattern. It is characterized by the presence of pigmented streaks in a radial arrangement at the edge of a given pigmented skin lesion.
- Parallel pattern. It is found exclusively in melanocytic lesions on skin of palms and soles due to particular anatomic structures inherent to this location.
- Multicomponent pattern. It is a combination of three or more distinctive dermoscopic structures within a given lesion.
- Lacunar pattern. It is characterized by various to numerous, smooth-bordered, round to oval, variously sized structures called red lacunas, whose morphologic hallmark is their reddish, blue-purplish or black coloration.
- Unspecific pattern. In some instances, a pigmented lesion cannot be categorized into one of the global patterns listed above, because its overall morphologic aspect

does not fit at all into these artificial, albeit rather distinctive categories. For this type of lesion the term unspecific pattern is used.

In [51] and [52] Tanaka et al. presented an analysis of texture to classify a pattern into three categories: homogeneous, globular and reticular. The lesion area was divided into small regions. 110 texture features of each sub-image were calculated. These features were based on intensity histogram information, differential statistical features, Fourier power spectrum, run-length matrix, cooccurrence matrix and connected components. 35 features were selected by discriminant analysis. As result, the patterns could be classified correctly into three categories at the ratio of 94% of classification success rate.

In [44] Serrano and Acha proposed a model-based technique to automatically classify five types of global patterns (reticular, globular, cobblestone, homogeneous and parallel). In the model-based methods, image classification was treated as an incomplete data problem, where the value of each pixel was known and the label, which designated the texture pattern the pixel belongs to, is missing. In such techniques, images were modelled as random fields and the segmentation/classification problem was posed as an statistical optimization problem. Most of the existing techniques use the spatial interaction models like Markov Random Field (MRF) or Gibbs Random Field (GRF) to model digital images. Following Xia et al. model [55], Serrano and Acha considered an image as a random field G , defined on a $W \times H$ rectangular lattice, where W and H represented the image dimensions. The lattice was denoted by $S = \{(i, j) : 1 \leq i \leq W, 1 \leq j \leq H\}$, which was indexed by the coordinate (i, j) . The color values were represented by $G = \{\mathbf{G}_s = \mathbf{g}_s : s \in S\}$, where $s = (i, j)$ denoted a specific site and the random variable \mathbf{G}_s represented a color pixel in the $L^*a^*b^*$ color space. An observed image was an instance of G . It could be described by a finite symmetric conditional model (FSCM) [28] as follows:

$$\mathbf{g}_s = \mu_s + \sum_{t \in \nu_g} \beta_{s,t}[(\mathbf{g}_{s+t} - \mu_{s+t}) + (\mathbf{g}_{s-t} - \mu_{s-t})] + \mathbf{e}_s \quad (1)$$

where $\nu_g = \{(0, 1), (1, 0), (1, 1), (-1, 1)\}$ is the set of shift vectors corresponding to the second order neighbourhood system, $\mu_s = [\mu_L, \mu_a, \mu_b]^T$ is the mean of the color pixels in a window centred in site s , $\{\beta_{s,t} : t \in \nu_g\}$ is a diagonal matrix whose elements are the set of correlation coefficients associated with the set of translations from the central site s and $\{\mathbf{e}_s\}$ is a stationary Gaussian noise color sequence with a diagonal covariance matrix Σ as:

$$\Sigma = \begin{bmatrix} \sigma_L^2 & 0 & 0 \\ 0 & \sigma_a^2 & 0 \\ 0 & 0 & \sigma_b^2 \end{bmatrix} \quad (2)$$

Thus, an 18-component feature vector characterized the random field G :

$$\mathbf{f} = (\mu_L, \mu_a, \mu_b, \sigma_L^2, \sigma_a^2, \sigma_b^2, \beta_{L,t}, \beta_{a,t}, \beta_{b,t} : t \in \nu_g) \quad (3)$$

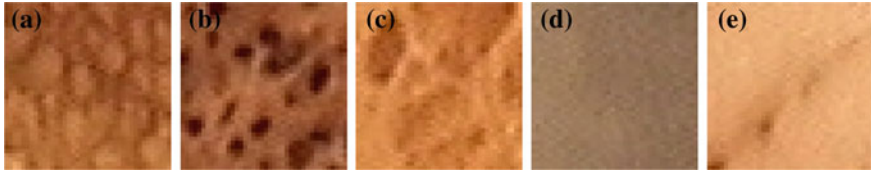


Fig. 8 Example of global patterns. 40×40 dermoscopic image sample representing global patterns: **a** reticular pattern; **b** globular pattern; **c** cobblestone pattern; **d** homogeneous pattern and **(e)** parallel pattern

In order to estimate the parameter vector \mathbf{f} , the least-squares estimation method was applied.

Features were supposed to follow a Normal mixture distribution, with a different mean vector and covariance matrix depending on the global pattern each particular image was representing. In other words, if λ represented the pattern class, features will follow the distribution:

$$N(\mathbf{M}_\lambda, \Sigma_\lambda) = \frac{1}{\sqrt{(2\pi)^n |\Sigma_\lambda|}} \exp \left(-\frac{1}{2} (\mathbf{f} - \mathbf{M}_\lambda)^T \Sigma_\lambda^{-1} (\mathbf{f} - \mathbf{M}_\lambda) \right) \quad (4)$$

In order to find the optimum label the pattern belongs to, the *maximum a-posteriori* (MAP) criterion was applied together with the assumption that the five possible global patterns (reticular, cobblestone, homogeneous, parallel and globular) were equally probable, what resulted in the *maximum likelihood* (ML) criterion. Then:

$$\hat{\lambda} = \arg \max_{\lambda \in \Lambda} P(\mathbf{F} = \mathbf{f} | \lambda) \quad (5)$$

This ML problem can then be solved by minimizing the following energy:

$$\hat{\lambda} = \min_{\lambda \in \Lambda} E_G(\mathbf{f}, \lambda) = \min_{\lambda \in \Lambda} \{ ((\mathbf{f} - \mathbf{M}_\lambda)^T \Sigma_\lambda^{-1} (\mathbf{f} - \mathbf{M}_\lambda) + \ln \left((2\pi)^{18} |\Sigma_\lambda| \right) \} \quad (6)$$

The proposed algorithm was tested on a database containing 100 40×40 image samples of the five types of patterns (see Fig. 8). For each type of them 20 images were used. 10-fold cross-validation was performed: 90 % of the total set of images was used to train (90 images) and 10 % to validate (10 images). The total set was divided into 10 groups for the testing. Each time one different testing group was employed to validate the algorithm. In this way, 18 images of each pattern were used to train and two images of each type were used to validate. The authors compared different color spaces obtaining the success classification percentages described in Table 8.

Since Serrano and Acha developed their methodology to analyze global pattern in pigmented lesions in 2009, different researchers have followed their steps.

Gola et al. [25] presented a method which, in conjunction with the ABCD rule, tried to detect three global patterns in order to increase diagnostic accuracy of pigmented

Table 8 Percentage of success clasification in five global patterns for different color spaces

	Reticular	Globular	Cobblestone	Homogeneous	Parallel	Average
RGB	85	85	50	95	85	80
YIQ	75	90	70	95	70	80
HSV	70	80	65	95	95	81
L*a*b*	90	80	80	90	90	86

lesions. To this aim they developed three different algorithms. In the two first ones, based on edge detection and mathematical morphology, they detected globular and reticular patterns. In the third one, they performed color analysis in the RGB color space with the aim of detecting the blue veil pattern. The algorithms were tested with a database consisting of 20 images per global pattern. The proposed algorithms produced an average accuracy above 85 %.

In [40] the authors detected and classified global dermoscopic patterns as well. They investigated texture analysis and classified five classes of global lesion patterns (reticular, globular, cobblestone, homogeneous, and parallel ones). To this purpose, a statistical approach based on texton classification was followed, where texture features were modelled by the joint probability distribution of filter responses. This distribution was represented by texton (cluster center) frequencies, and textons and texture models were learnt from training images. The classification of an unseen image proceeded by mapping the image to a texton distribution and comparing this distribution to the learnt models. The texton-based classification was performed in the L*a*b* color space and in the gray-scale image using different filter banks. The procedure was divided into two steps:

- Learning stage
 1. A set of 81×81 pixel images representing the five patterns were assembled.
 2. Training images were convolved with a filter bank to generate filter responses.
 3. Exemplar filter responses were chosen as textons and were used to label each filter response in the training images.
 4. The histogram of texton frequencies was used to form models corresponding to the training images.
- Classification stage
 1. The same procedure as in the training stage was followed to build the histogram corresponding to the unseen image.
 2. This histogram was then compared with the models of the texton dictionary.
 3. A nearest neighbor classifier was used and the Chi-square statistic was employed to measure distances.

The proposed set of filters was a filter bank composed by $18 + 18 + 2$ filters to detect average intensity, edges, spots, wave, meshes and ripples of dermatoscopic structures. The correct classification rate attained was 86.8 %.

Table 9 Classification results in [1]

Pattern	SE (%)	SP (%)	AUC
Reticular	87.11	97.96	0.981
Globular	86.25	97.21	0.997
Cobblestone	87.76	93.23	0.990
Homogeneous	90.47	95.10	0.996
Parallel	85.25	89.50	0.989
Starburst	89.62	90.14	0.966
Multicomponent	98.50	93.11	0.989

SE Sensitivity, SP specificity, AUC Area under the Receiver operating characteristic (ROC) curve

Table 10 Classification results in [27]

Classifier	SE (%)	SP (%)	AUC
Melanoma	100	95.9	0.993
Parallel ridge pattern	93.1	97.7	0.985
Parallel furrow pattern	90.4	85.9	0.931
Fibrillar pattern	88	77.9	0.89

SE Sensitivity, SP specificity, AUC Area under the Receiver operating characteristic (ROC) curve

In their work, Abbas et al. [1] extracted color and texture features from the dermoscopic image in order to classify it into its global pattern. Color related images were extracted from the CIECAM02 representation of the color image. Texture was analysed by means of the steerable pyramids transform (SPT). Both groups of features fed an AdaBoost MC classifier, which classified pigmented lesions into seven different groups of global patterns: (a) Reticular pattern or pigmented network, (b) Globular pattern, (c) Cobblestone pattern, (d) Homogeneous pattern, (e) Parallel pattern, (f) Starburst pattern, (g) Multicomponent pattern. In Table 9 results are summarized.

Iyatomi et al. [27] focused only on the detection of parallel pattern. 428 image features were extracted, which included color-related features, symmetry features, border-related features and texture features. Then, using principal component analysis (PCA), these features were transformed into 198 orthogonal principal components (PCs) without information loss. The first 10 PCs more discriminative were selected. Four linear classifiers were used for parallel ridge, parallel furrow and fibrillar pattern detection. In addition, acral volar melanoma was also classified. The achieved results are shown in Table 10.

Discussion

Pattern analysis is the method most commonly used for providing diagnostic accuracy for cutaneous melanoma [38]. In fact, it was deemed superior to the other algorithms (i.e., ABCD Dermoscopy Rule, Menzies score, 7-Point Checklist) for diagnostic

efficiency by experts from all over the world in the 2000 Consensus Net Meeting on Dermoscopy (CNMD) [5].

Pattern analysis aims to detect local or global patterns in a pigmented lesion to determine if it is melanocytic and, in such a case, its malignancy [5]:

1. Detection of pigment network, aggregate globules, streaks, homogeneous blue or parallel pattern are signs of melanocytic lesions.
2. Atypical pigment network, dots or streaks irregularly distributed, blue-white veil or regression may be signs of melanoma.

The presence of specific dermoscopic features in different regions of the same lesion contributes to make a diagnosis of melanocytic lesions and these features are called local patterns. The predominant presence of some of these local patterns determines some global patterns.

In the literature, much more works devoted to detect local patterns than global patterns are published. Most of the papers related to local patterns address the problem of the detection of the pigmented network, which is the most common local pattern appearing in melanocytic lesions.

Regarding global patterns, Serrano's article [44] was the first work that automatically detected global patterns in dermoscopic images. Nevertheless, multicomponent pattern was not considered in this paper. Later, other works have provided new methods to classify global patterns, included multicomponent, with high success classification rate.

References

1. Abbas, Q., Celebi, M.E., Serrano, C., Garcia, I.F., Ma, G.: Pattern classification of dermoscopy images: a perceptually uniform model. *Pattern Recognit.* **46**, 86–97 (2013)
2. Anantha, M., Moss, R.H., Stoecker, W.V.: Detection of pigment network in dermatoscopy images using texture analysis. *Comput. Med. Imaging Graph.* **28**(5), 225–234 (2004)
3. Argenziano, G., Fabbrocini, G., Carli, P., De Giorgi, V., Sammarco, E., Delfino, M.: Epiluminescence microscopy for the diagnosis of doubtful melanocytic skin lesions. Comparison of the ABCD rule of dermatoscopy and a new 7-point checklist based on pattern analysis. *Arch. Dermatol.* **134**, 1563–1570 (1998)
4. Argenziano, G., Soyer, H., De Giorgi, V., Piccolo, D., Carli, P., Delfino, M., Ferrari, A., Hofmann-Wellenhof, R., Massi, D., Mazzocchetti, G., Scalvenzi, M., Wolf, I.H.: *Interactive atlas of dermoscopy*. EDRA-Medical Publishing and New Media, Milan (2000)
5. Argenziano, G., Soyer, H.P., Chimenti, S., Talamini, R., Corona, R., Sera, F., Binder, M., Kopf, A.W.: Dermoscopy of pigmented skin lesions: results of a consensus meeting via the internet. *J. Am. Acad. Dermatol.* **48**(5), 680–693 (2003)
6. Arroyo, J. L. G., Zapirain, B. G., Zorrilla, A. M.: Blue-white veil and dark-red patch of pigment pattern recognition in dermoscopic images using machine-learning techniques. In: *IEEE International Symposium on Signal Processing and Information Technology, ISSPIT 2011*, art. no. 6151559, 196–201 (2011)
7. Barata, C., Marques, J. S., Rozeira, J.: A system for the detection of pigment network in dermoscopy images using directional filters. *IEEE Trans. Biomed. Eng.* **59**(10), art. no. 100, 2744–2754 (2012)

8. Betta, G., Di Leo, G., Fabbrocini, G., Paolillo, A., Scalvenzi, M.: Automated application of the “7-point checklist” diagnosis method for skin lesions: estimation of chromatic and shape parameters. Conference Record —IEEE Instrumentation and Measurement Technology Conference 3, art. no. 1604486, 1818–1822 (2005)
9. Betta, G., Di Leo, G., Fabbrocini, G., Paolillo, A., Sommella, P.: Dermoscopic image-analysis system: estimation of atypical pigment network and atypical vascular pattern. IEEE International Workshop on Medical Measurement and Applications, MeMeA, art. 1644462, 63–67 (2006)
10. Braun, R.P., Rabinovitz, H.S., Oliviero, M., Kopf, A.W., Saurat, J.-H.: Dermoscopy of pigmented skin lesions. *J. Am. Acad. Dermatol.* **52**(1), 109–121 (2005)
11. Capdehourat, G., Corez, A., Bazzano, A., Alonso, R., Musé, P.: Toward a combined tool to assist dermatologists in melanoma detection from dermoscopic images of pigmented skin lesions. *Pattern Recognit. Lett.* **32**, 2187–2196 (2011)
12. Celebi, M. E., Kingravi, H. A., Aslandogan, Y. A., Stoecker, W. V.: Detection of blue–white veil areas in dermoscopy images using machine learning techniques. *Progress in Biomedical Optics and Imaging—proceedings of SPIE 6144 III*, art. no. 61445T (2006)
13. Celebi, M.E., Iyatomi, H., Stoecker, W.V., Moss, R.H., Rabinovitz, H.S., Argenziano, G., Soyer, H.P.: Automatic detection of blue–white veil and related structures in dermoscopy images. *Comput. Med. Imaging Graph.* **32**(8), 670–677 (2008)
14. Celebi, M.E., Stoecker, W.V., Moss, R.H.: Advances in skin cancer image analysis. *Comput. Med. Imaging Graph.* **35**(2), 83–166 (2011)
15. Dalal, A., Moss, R.H., Stanley, R.J., Stoecker, W.V., Gupta, K., Calcara, D.A., Xu, J., Shrestha, B., Drugge, R., Malter, J.M., Perry, L.A.: Concentric decile segmentation of white and hypopigmented areas in dermoscopy images of skin lesions allows discrimination of malignant melanoma. *Comput. Med. Imaging Graph.* **35**(2), 148–154 (2011)
16. Di Leo G., Paolillo A., Sommella, P., Fabbrocini, G., Rescigno, O.: A software tool for the diagnosis of melanomas. In: 2010 IEEE Instrumentation and Measurement Technology Conference, pp. 886–891 (2010)
17. Di Leo, G., Fabbrocini, G., Paolillo, A., Rescigno, O., Sommella, P.: Toward an automatic diagnosis system for skin lesions: estimation of blue–whitish veil and regresin structures. In: 6th International Multi-Conference on Systems, Signals and Devices (2009)
18. Di Leo, G., Fabbrocini, G., Paolillo, A., Sommella, P.: Automatic Diagnosis of Melanoma: a Software System based on the 7-Point Check- List. In: Proceedings of the 43rd Annual Hawaii International Conference on System Sciences, 5–8 Jan, Computer Society Press (2010)
19. Di Leo, G., Paolillo, A., Sommella, P., Liguori, C.: An improved procedure for the automatic detection of dermoscopic structures in digital ELM images of skin lesions. In: Proceedings of IEEE Conference Virtual Environments Human-Computer Interfaces and Measurement Systems, pp. 190–194 (2008)
20. Fabbrocini, G., Betta, G., Di Leo, G., Liguori, C., Paolillo, A., Pietrosanto, A., et al.: Epiluminescence image processing for melanocytic skin lesion diagnosis based on 7-point check-list: a preliminary discussion on three parameters. *Open Dermatol. J.* **2010**(4), 110–115 (2010)
21. Fleming, M.G., Steger, C., Zhang, J., Gao, J., Cognetta, A.B., Pollak, L., Dyer, C.R.: Techniques for a structural analysis of dermatoscopic imagery. *Comput. Med. Imaging Graph.* **22**(5), 375–389 (1998)
22. Frangi, A., Niessen, W.J., Vincken, K.L., Viergever, M.A.: Multiscale vessel enhancement filtering. In: Wells, W.M., Colchester, A.C.F., Delp, S.L. (eds.) *MICCAI*, pp. 130–137. Springer, Heidelberg (1998)
23. Grana, C., Cucchiara, R., Pellacani, G., Seidenari, S.: Line detection and texture characterization of network patterns. In: Proceedings—International Conference on Pattern Recognition, vol. 2(1699200), pp. 275–278 (2006)
24. Hanmandlu, M., Seba, S., Madasu, V.K., Lovell, B. C.: Fuzzy co-clustering of medical images using Bacterial Foraging. In: 23rd International Conference Image and Vision Computing New Zealand, pp. 1–6. IEEE press, New York (2008)

25. Isasi Gola, A., Garcia Zapirain, B., Mendez Zorrilla, A.: Melanomas non-invasive diagnosis application based on the ABCD rule and pattern recognition image processing algorithms. *Comput. Biol. Med.* **41**, 742–755 (2011)
26. Iyatomi, H., Oka, H., Celebi, M.E., Tanaka, M., Ogawa K.: Parameterization of dermoscopic findings for the internet-based melanoma screening system. In: *Proceedings of the 2007 IEEE Symposium on Computational Intelligence in Image and Signal Processing (CIISP 2007)*, pp. 189–193 (2007)
27. Iyatomi, H., Oka, H., Celebi, M.E., Ogawa, K., Argenziano, G., Soyer, H.P., Koga, H., Saida, T., Ohara, K., Tanaka, M.: Computer-based classification of dermoscopy images of melanocytic lesions on acral volar skin. *J. Invest. Dermatol.* **128**(8), 2049–2054 (2008)
28. Kashyap, R.: Chellappa, R.: Estimation and choice of neighbors in spatial interaction models of images. *IEEE Trans. Inf. Theory* **1**, 60–72 (1983)
29. Kass, M., Witkin, A.: Analyzing oriented patterns. *Comput. Vis. Graph. Image Proces.* **37**(3), 362–385 (1987)
30. Khan, A., Gupta, K., Stanley, R.J., Stoecker, W.V., Moss, R.H., Argenziano, G., Soyer, H.P., Cognetta, A.B.: Fuzzy logic techniques for blotch feature evaluation in dermoscopy images. *Comput. Med. Imaging Graph.* **33**(1), 50–57 (2009)
31. Korotkov, K., Garcia, R.: Computerized analysis of pigmented skin lesions: a review. *Artif. Intel. Med.* **56**(2), 69–90 (2012)
32. Madasu, V. K., Lovell, B.C.: Blotch detection in pigmented skin lesions using fuzzy co-clustering and texture segmentation. *DICTA 2009—Digital Image Computing: Techniques and Applications*, art. no. 5384959, 25–31 (2009)
33. Maglogiannis, I., Doukas, C.N.: Overview of advanced computer vision systems for skin lesions characterization. *IEEE Trans. Inf. Technol. Biomed.* **13**(5), 721–733 (2009)
34. Mirzaalian, H., Lee, T.K., Hamarneh, G.: Learning features for streak detection in dermoscopic color images using localized radial flux of principal intensity curvature. In: *Proceedings of the Workshop on Mathematical Methods in Biomedical Image Analysis*, 6164758, pp. 97–101 (2012)
35. Ojala, T., Pietikainen, M., Maenpaa, T.: Multiresolution gray-scale and rotation invariant texture classification with local binary patterns. *IEEE Trans. Pattern Anal. Mach. Intel.* **24**(7), 971–987 (2002)
36. Pehamberger, H., Steiner, A., Wolff, K.: In vivo epiluminescence microscopy of pigmented skin lesions. I. Pattern analysis of pigmented skin lesions. *J. Am. Acad. Dermatol.* **17**, 571–583 (1987)
37. Rangayyan, R.M., Acha, B., Serrano, C.: *Color image processing with biomedical applications*. SPIE Press, Bellingham (2011)
38. Rezze, G.G., De Sa, B.C.S., Neves, R.I.: Dermoscopy: the pattern analysis. *Anais Brasileiros de Dermatologia* **81**(3), 261–268 (2006)
39. Sadeghi, M., Lee, T., Lui, H., McLean, D., Atkins, S.: Detection and analysis of irregular streaks in dermoscopic images of skin lesions. *IEEE Trans. Med. Imaging* (2013, in press)
40. Sadeghi, M., Lee, T.K., McLean, D., Lui, H., Atkins, M.S.: Global pattern analysis and classification of dermoscopic images using textons. *Progress in Biomedical Optics and Imaging—Proceedings of SPIE 8314*, art. no. 83144X (2012)
41. Sadeghi, M., Lee, T.K., McLean, D., Lui, H., Atkins, M.S.: Oriented pattern analysis for streak detection in dermoscopy images. *Medical image computing and computer-assisted intervention : MICCAI*. In: *International Conference on Medical Image Computing and Computer-Assisted Intervention*, 15(Pt 1), pp. 298–306 (2012)
42. Sadeghi, M., Razmara, M., Wighton, P., Lee, T.K., Atkins, M.S.: Modeling the dermoscopic structure pigment network using a clinically inspired feature set. *Lecture Notes in Artificial Intelligence and Lecture Notes in Bioinformatics. LNCS*, vol. 6326, pp. 467–474. Springer, New York (2010)
43. Sadeghi, M., Razmara, M., Lee, T.K., Atkins, M.S.: A novel method for detection of pigment network in dermoscopic images using graphs. *Comput. Med. Imaging Graph.* **35**(2), 137–143 (2011)

44. Serrano, C., Acha, B.: Pattern analysis of dermoscopic images based on Markov random fields. *Pattern Recognit.* **42**, 1052–1057 (2009)
45. Shrestha, B., Bishop, J., Kam, K., Chen, X., Moss, R.H., Stoecker, W.V., Umbaugh, S., Stanley, R.J., Celebi, M.E., Marghoob, A.A., Argenziano, G., Soyer, H.P.: Detection of atypical texture features in early malignant melanoma. *Skin Res. Technol.* **16**(1), 60–65 (2010)
46. Situ, N., Yuan, X., Zouridakis, G.: Boosting instance prototypes to detect local dermoscopic features. In: 2010 Annual International Conference of the IEEE Engineering in Medicine and Biology Society, EMBC'10, art. no. 5626776, pp. 5561–5564 (2010)
47. Skrovseth, S.O., Schopf, T.R., Thon, K., Zortea, M., Geilhufe, M., Mllersen, K., Kirchesch, H.M., Godtliebsen, F.: A computer aided diagnostic system for malignant melanomas. In: 2010 3rd International Symposium on Applied Sciences in Biomedical and Communication Technologies. ISABEL, 2010, 5702825 (2010)
48. Steger, C.: An unbiased detector of curvilinear structures. *IEEE Trans. Pattern Anal. Mach. Intel.* **20**(2), 113–125 (1998)
49. Stoecker, W.V., Moss, R.H.: Editorial: digital imaging in dermatology. *Comput. Med. Imaging Graph.* **16**(3), 145–150 (1992)
50. Stoecker, W.V., Gupta, K., Stanley, R.J., Moss, R.H., Shrestha, B.: Detection of asymmetric blotches (asymmetric structureless areas) in dermoscopy images of malignant melanoma using relative color. *Skin Res. Technol.* **11**(3), 179–184 (2005)
51. Tanaka, T., Torii, S., Kabuta, I., Shimizu, K., Tanaka, M., Oka, H.: Pattern classification of nevus with texture analysis. In: Annual International Conference of the IEEE Engineering in Medicine and Biology—Proceedings 26 II, pp. 1459–1462 (2004)
52. Tanaka, T., Torii, S., Kabuta, I., Shimizu, K., Tanaka, M.: Pattern classification of nevus with texture analysis. *IEEE Trans. Electr. Electron. Eng.* **3**(1), 143–150 (2008)
53. Wighton, P., Lee, T.K., Lui, H., McLean, D.I., Atkins, M.S.: Generalizing common tasks in automated skin lesion diagnosis. *IEEE Trans. Information Technology in Biomed.* **15**(4), 5763779, 622–629 (2011)
54. Wighton, P., Sadeghi, M., Lee, T.K., Atkins, M.S.: A fully automatic random walker segmentation for skin lesions in a supervised setting. *Lecture Notes in Computer Science (including subseries Lecture Notes in Artificial Intelligence and Lecture Notes in Bioinformatics)*, LNCS (PART 2), vol. 5762, pp. 1108–1115. Springer, Heidelberg (2009)
55. Xia, Y., Feng, D., Zhao, R.: Adaptive segmentation of textured images by using the coupled Markov random field model. *IEEE Trans. Image Proces.* **11**, 3559–3566 (2006)
56. Yoshino, S., Tanaka, T., Tanaka, M., Oka, H.: Application of morphology for detection of dots in tumor. In: Proceedings of the SICE Annual Conference, WPI-3-3, pp. 407–410 (2004)

Computer Vision Techniques for the Diagnosis of Skin
Cancer

Scharcanski, J.; Celebi, M.E. (Eds.)

2014, X, 282 p. 136 illus., 120 illus. in color., Hardcover

ISBN: 978-3-642-39607-6